Urania
Jurnal Ilmiah Daur Bahan Bakar Nuklir

Beranda jurnal: http://jurnal.batan.go.id/index.php/urania/

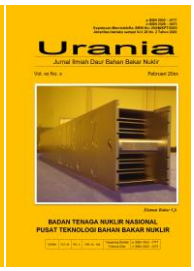

EFFECT OF Al, Zr AND Mo ON CORROSION RESISTANCE OF $Al_xCrFeNiMo$ AND $Al_xCrFeNiZr$ (X = 1, 1.2 AND 1.4) AS NUCLEAR FUEL CLADDING MATERIALS

Teguh Firmansyah[1], Bonita Dilasari[1], Jan Setiawan[2], Djoko Hadi Prajitno[3]
[1]Department of Metallurgical Engineering, Bandung Institute of Technology,
Bandung, West Java, Indonesia, 40132
[2]Research Center for Advanced Materials – BRIN
PUSPIPTEK Area, Serpong, Tangerang Selatan, Banten, Indonesia, 15314
[3]Research Center for Radiation Process – BRIN
Bandung, West Java, Indonesia, 40132
e-mail: teguhfirmansyah268@gmail.com

(Naskah diterima: 07–02–2022, Naskah direvisi: 17–02–2022, Naskah disetujui: 25–02–2022)

ABSTRACT

EFFECT OF Al, Zr AND Mo ON CORROSION RESISTANCE OF $Al_xCrFeNiMo$ AND $Al_xCrFeNiZr$ (X=1, 1.2 AND 1.4) AS FUEL CLADDING MATERIALS. The high entropy alloy of $Al_xCrFeNiM$ (with x = 1, 1,2 and 1,4; M = Mo and Zr) was successfully synthesized using powder metallurgy technique with sintering process at 1000 ^oC in an inert atmosphere. These alloys were designated as fuel cladding for research reactor with high U-density fuel such as U-Mo. One of the critical in-service properties of nuclear fuel cladding is its corrosion behavior. In this study, some properties of the HEA of $Al_xCrFeNiM$ such as the phases, microstructures, hardness, and corrosion resistance in 3 wt.% NaCl solution at room temperature were investigated. The results show that the phases in the HEA of $Al_xCrFeNiMo$ are FeNi, AlNi and Mo. The HEA of $Al_xCrFeNiZr$ has more complex phases compared to the $Al_xCrFeNiMo$. The microstructure of HEA samples show fine grains with some micropores that imperfect the solidification during the sintering process. The hardness value of the HEA of $Al_xCrFeNiMo$ has a trend of decreasing as the x value increases. The opposite trend occurs to the HEA of $Al_xCrFeNiZr$ that the hardness value increases with increasing x value. The lowest hardness value is $Al_{1.4}CrFeNiMo$ at 262.2 HV, and the highest hardness value of $Al_{1.4}CrFeNiZr$ is at 756.7 HV. The corrosion rate of the $Al_xCrFeNiMo$ does not show a specific trend with increasing x value; however, the $Al_xCrFeNiZr$ shows decreasing value with increasing x value. The lowest value for the all-HEA samples is 0.20 mmpy for the $Al_{1.4}CrFeNiZr$. The results of hardness and corrosion tests show that the Zr element combined with the Al element affects not only its hardness but also its corrosion resistance.

Keywords: Fuel cladding, high entropy alloy, corrosion.

.

ABSTRAK

PENGARUH Al, Zr DAN Mo TERHADAP KETAHANAN KOROSI $Al_XCrFeNiMo$ DAN $Al_XCrFeNiZr$ (X=1, 1,2 DAN 1,4) SEBAGAI MATERIAL KELONGSONG NUKLIR. *Paduan entropi tinggi $Al_xCrFeNiM$ (with x = 1, 1.2 and 1.4) disintesis menggunakan teknik metalurgi bubuk dengan proses sinter pada suhu 1000^{o}C. Paduan ini didesain sebagai kelongsong bahan bakar untuk reaktor riset dengan densitas U yang tinggi seperti U-Mo. Salah satu sifat penting kelongsong bahan bakar nuklir adalah ketahanan korosi. Pada studi ini, beberapa sifat dari sampel HEA $Al_xCrFeNiM$ seperti fasa, struktur mikro, kekerasan, dan ketahanan korosi dalam larutan 3% berat NaCl pada temperatur kamar diselidiki. Hasil studi menunjukkan fasa sampel HEA $Al_xCrFeNiMo$ adalah FeNi, AlNi, dan Mo. Sampel HEA $Al_xCrFeNiZr$ lebih kompleks jika dibandingkan dengan $Al_xCrFeNiMo$. Struktur mikro dari sampel HEA menunjukkan butiran halus dengan beberapa mikropori karena pemadatan yang tidak sempurna selama proses sintering. Nilai kekerasan $Al_xCrFeNiMo$ cenderung turun seiring dengan peningkatan nilai x. Berbeda dengan $Al_xCrFeNiZr$ nilai kekerasan meningkat seiring dengan peningkatan nilai x. Nilai kekerasan terendah diperoleh sampel $Al_{1.4}CrFeNiMo$ sebesar 262,2 HV, dan nilai kekerasan tertinggi pada $Al_{1.4}CrFeNiZr$ dengan nilai 756,7 HV. Laju korosi sampel $Al_xCrFeNiMo$ tidak kecenderungan tertentu seiring dengan peningkatan nilai x, berbeda dengan $Al_xCrFeNiZr$ yang menunjukkan penurunan laju korosi seiring dengan peningkatan nilai x. Nilai terendah untuk semua sampel HEA adalah 0,20 mmpy pada sampel $Al_{1.4}CrFeNiZr$. Hasil kekerasan dan korosi menunjukkan bahwa unsur Zr yang dikombinasikan dengan unsur Al tidak hanya mempengaruhi kekerasannya tetapi juga ketahanan korosinya.*

Kata kunci*: Kelongsong, paduan entropi tinggi, korosi*

DOI: 10.17146/urania. 2022.28.1.6624

p ISSN: 0852-4777
e ISSN: 2528-0473

INTRODUCTION

GA Siwabessy Multipurpose Reactor (RSG-GAS) is a research reactor of the type currently used to development of nuclear fuel energy in Indonesia. RSG-GAS is reactor for the irradiation of materials and utilization of neutron flux through a beam tube where the irradiation is used to produce radioisotopes[1]. The nuclear fuel meat is containment by cladding materials. The temperature of nuclear fuel is relatively high because heat was generated due to nuclear chain reaction. The cooling system for RSG-GAS is using water with natural convection that can reduce the temperature of nuclear fuel through its cladding during operation. Nuclear fuel cladding in the reactor will be contacted and immersed in water for a long time so the cladding material must have a good corrosion resistance so that there is no degradation of the material from the cladding which can cause a particle from nuclear fuel and its cladding, and radiation leakage.

An alloy that has potential as materials candidate for nuclear fuel cladding is high entropy alloy (HEA). HEA is an alloy consisting of five or more elements with almost the same atomic percent and has a very high entropy of mixing value compared to conventional alloys, it makes HEA has a good microstructure and special properties such as high hardness and good corrosion resistance [2–5]. The elements used in HEA have an important role in the formation of special properties of the alloy where certain elements will increase the hardness and corrosion resistance of the alloy[6].

In this research, the HEA samples was produced by powder metallurgy technique with vary in Al content with the fitfth elements used are Zr and Mo. Calculation of the weight of the alloying elements used in the alloy sample was claculated considers the value of the relative atomic mass (Ar) and the number of moles of each element[7]. Physical properties and corrosion rates HEA samples were studied using Optical Microscopy, Scanning Electron Microscopy- Energy Dispersive Spectroscopy (SEM-EDS), X-Ray Diffraction (XRD), and density test using an autopycnometer. This study aimed to identify the phases, microstructure, mechanical properties, and corrosion rate in 3wt% NaCl solution of HEA samples AlCrFeNiMo, $Al_{1.2}$CrFeNiMo, $Al_{1.4}$CrFeNiMo AlCrFeNiZr, $Al_{1.2}$CrFeNiZr, and $Al_{1.4}$CrFeNiZr.

METHODOLOGY

a. Synthesis of High Entropy Alloy

The HEA of AlCrFeNiMo, $Al_{1.2}$CrFeNiMo, $Al_{1.4}$CrFeNiMo AlCrFeNiZr, $Al_{1.2}$CrFeNiZr, and $Al_{1.4}$CrFeNiZr produce by powder metallurgy. Each consisting elements is calculated by the weight percent required for each alloy, as presented in Table 1. After weighing, each element in powder form (Merck with 99% purity) was put into a ball mill and rotated for 15 minutes to have a homogeneous mixture. The homogeneous mixture powder continued to form into pellets with a diameter of 1.1 cm, a thickness of 0.3 mm, and a weight of 3 grams. The sample in the form of pellets continued by sintering at a temperature of 1000 ^oC for 1 hour using a tube furnace in inert atmosphere.

Table.1 Atomic percent and weight percent of the elements of the HEA sample

HEA	Element	Atomic (%)	Weight (%)
AlCrFeNiMo	Al	20	9.32
	Cr	20	17.96
	Fe	20	19.28
	Ni	20	20.27
	Mo	20	33.15
$Al_{1.2}$CrFeNiMo	Al	23.1	10.98
	Cr	19.2	17.63
	Fe	19.2	18.93
	Ni	19.2	19.91
	Mo	19.2	32.55
$Al_{1.4}$CrFeNiMo	Al	25.9	12.58
	Cr	18.5	17.31
	Fe	18.5	18.58
	Ni	18.5	19.55
	Mo	18.5	31.96
AlCrFeNiZr	Al	20	9.47
	Cr	20	18.26
	Fe	20	19.60
	Ni	20	20.61
	Zr	20	32.04
$Al_{1.2}$CrFeNiZr	Al	23.1	11.16
	Cr	19.2	17.92
	Fe	19.2	19.24
	Ni	19.2	20.23
	Zr	19.2	31.45
$Al_{1.4}$CrFeNiZr	Al	25.9	12.78
	Cr	18.5	17.59
	Fe	18.5	18.88
	Ni	18.5	19.86
	Zr	18.5	30.87

b. Characterization

Phases analysis of samples AlCrFeNiMo, $Al_{1.2}$CrFeNiMo, $Al_{1.4}$CrFeNiMo AlCrFeNiZr, $Al_{1.2}$CrFeNiZr, and $Al_{1.4}$CrFeNiZr, were carried out by Panalytical Empyrean Diffractometer, with a Cobalt anode for X-ray sources. the GSAS (General Structure Analysis Software) application was used for Rietveld analysis to determine the phases from the results of the X-ray diffractogram. The optical microscope and SEM-EDS were used to analyze the microstructure of HEA and quantified the weights elements contents. The hardness testing was carried out in triples using Vickers Hardness LM800T with an indentation time of 10 seconds. Measurement of the corrosion rate of HEA samples AlCrFeNiMo, $Al_{1.2}$CrFeNiMo, $Al_{1.4}$CrFeNiMo AlCrFeNiZr, $Al_{1.2}$CrFeNiZr, and $Al_{1.4}$CrFeNiZr using a potentiostat (Gamry Reference 3000) with a three-electrode system where the platinum as a counter electrode, Ag/AgCl as the reference electrode and the sample is the working electrode. Analyze using the potentiodynamic polarization from the initial potential of -0.3 V vs. potential open circuit (E_{oc}) to the final potential of 0.3 vs. E_{oc} with a scan rate of 0.005 V/sec in 3wt% NaCl solution.

RESULTS AND DISCUSSION

a. Crystallite Size of HEA

Table 2 shows crystallite size of AlCrFeNiMo, $Al_{1.2}$CrFeNiMo, $Al_{1.4}$CrFeNiMo, AlCrFeNiZr, $Al_{1.2}$CrFeNiZr, dan $Al_{1.4}$CrFeNiZr HEA samples was carculated from X-ray diffractogram. The crystallite size was determined by correction factor which the presence of micro-strain in each sample used Williamson-Hall equation write as below [8]:

$$\beta \cos \theta = \frac{k\lambda}{D} + 4\varepsilon \sin \theta \quad (1)$$

The β is FWHM (Full Width at Half Maximum), where the equation shows a linear relationship between y (FWHM cos θ) and x (sin θ). The kλ/D is the intercept to the y axis and 4ε is the gradient of a straight-line equation. According to research by Rodriguez et al [9] explained that the crystallite size has an effected on the mechanical properties of alloy. The crystallite size value is influenced by the phase formed in the alloy [10]. The dominant phases consisting of Al and Ni elements tend to have smaller crystallite sizes than the phases consisting of Fe elements.

Table 2. Crystallite size of HEA samples

HEA	Crystallite Size (nm)
AlCrFeNiMo	16.83
$Al_{1.2}$CrFeNiMo	20.66
$Al_{1.4}$CrFeNiMo	22.05
AlCrFeNiZr	29.47
$Al_{1.2}$CrFeNiZr	28.88
$Al_{1.4}$CrFeNiZr	16.91

b. Phases of HEA

Table 3 shows the phases formed in the samples of AlCrFeNiMo, $Al_{1.2}$CrFeNiMo, $Al_{1.4}$CrFeNiMo, AlCrFeNiZr, $Al_{1.2}$CrFeNiZr, and $Al_{1.4}$CrFeNiZr. In the HEA samples with Mo element were identified the FeNi that match with ICSD 98-0103556 and AlNi that match with ICSD 98-060-4356. The γ-FeNi phase will be formed at temperature ranged 425 -1420 ^oC which has FCC crystal structure. However, in quenching equilibrium the phase can produce a crystal structure of BCC (α-Fe) depending on the ratio between Fe and Ni[11]. While the AlNi phase is formed at temperature range of 500-1600 ^oC with the same percentage of Al and Ni [12]. In the HEA sample using the Zr element, several phases were identified were composed of elements such as Al-Cr-Ni which were formed at temperature of 1000 ^oC[13]. While the phase consisting of Al-Ni-Zr elements is formed at temperature of 850 ^oC[14].

c. Microstructure of HEA

Figure 1 shows the surface microstructure of the HEA samples AlCrFeNiMo, $Al_{1.2}$CrFeNiMo, $Al_{1.4}$CrFeNiMo, AlCrFeNiZr, $Al_{1.2}$CrFeNiZr, and $Al_{1.4}$CrFeNiZr were analyzed at 500X magnification using an Optical Microscope. Results of optical microstructure shows the pores in HEA samples. According to An and Zhu [15] the formation of pores in HEA is caused by sintering at high temperatures, this causes air expansion on the surface of samples which triggers the formation of pores. Based on the results of optical microscopy shows that the $Al_{1.2}$CrFeNiMo sample had a different microstructure compared to the AlCrFeNiMo and $Al_{1.4}$CrFeNiMo samples, this was affected by the phase formed in the alloy that the $Al_{1.2}$CrFeNiMo sample have dominant FeNi and Mo phases as shown in Table 3.

DOI: 10.17146/urania.2021.27.2.6406

Table 3. Phases of HEA $Al_xCrFeNiMo$ and $Al_xCrFeNiZr$.

HEA	Phases	Space Group and Lattice Parameter	Weight (%)
AlCrFeNiMo	FeNi ICSD 98-010-3556	Fm-3m a=b=c (Å): 3.5	7.8
	Mo COD 96-901-2433	Im-3m a=b=c (Å): 3.1	2.0
	AlNi ICSD 98-060-4356	Pm-3m a=b=c (Å): 2.8	90.2
$Al_{1.2}CrFeNiMo$	FeNi ICSD 98-010-3556	Fm-3m a=b=c (Å): 3.6	43.3
	Mo COD 96-901-2433	Im-3m a=b=c (Å): 3.1	18.0
	AlNi ICSD 98-060-4356	Pm-3m a=b=c (Å): 2.8	38.7
$Al_{1.4}CrFeNiMo$	FeNi ICSD 98-010-3556	Fm-3m a=b=c (Å): 2.9	49.4
	Mo COD 96-901-2433	Im-3m a=b=c (Å): 3.1	11.5
	AlNi ICSD 98-060-4356	Pm-3m a=b=c (Å): 2.8	39.1
AlCrFeNiZr	AlCrNi ICSD 98-011-0813	Pm-3m a=b=c (Å): 2.8	30.9
	ZrNiAl ICSD 98-015-2131	P–62m a=b (Å): 6.9 c (Å): 3.4	10.8
	$AlNi_4Zr_5$ ICSD 98-041-5704	P 42/m a=b (Å): 7.2 c (Å): 6.5	24.0
	$AlNi_2Zr$ ICSD 98-005-8081	Fm-3m a=b=c (Å): 6,1	5.1
	Fe ICSD 98-005-3803	Fm-3m a=b=c (Å): 3.6	29.2
$Al_{1.2}CrFeNiZr$	AlCrNi ICSD 98-011-0813	Pm-3m a=b=c (Å): 2.8	27.6
	ZrNiAl ICSD 98-015-2131	P-62m a=b (Å): 6.9 c (Å): 3.4	19.8
	$AlNi_4Zr_5$ ICSD 98-041-5704	P 42/m a=b (Å): 7.2 c (Å): 6.7	51.5
	$AlNi_2Zr$ ICSD 98-005-8081	Fm-3m a=b=c (Å): 6.0	1.1
$Al_{1.4}CrFeNiZr$	AlCrNi ICSD 98-011-0813	Pm-3m a=b=c (Å): 2.8	75.3
	ZrNiAl ICSD 98-015-2131	P-62m a=b (Å): 6.8 c (Å): 3.4	5.8
	$AlNi_4Zr_5$ ICSD 98-041-5704	P 42/m a=b (Å): 7.1 c (Å): 6.5	16.3
	$AlNi_2Zr$ ICSD 98-005-8081	Fm-3m a=b=c (Å): 6.1	2.6

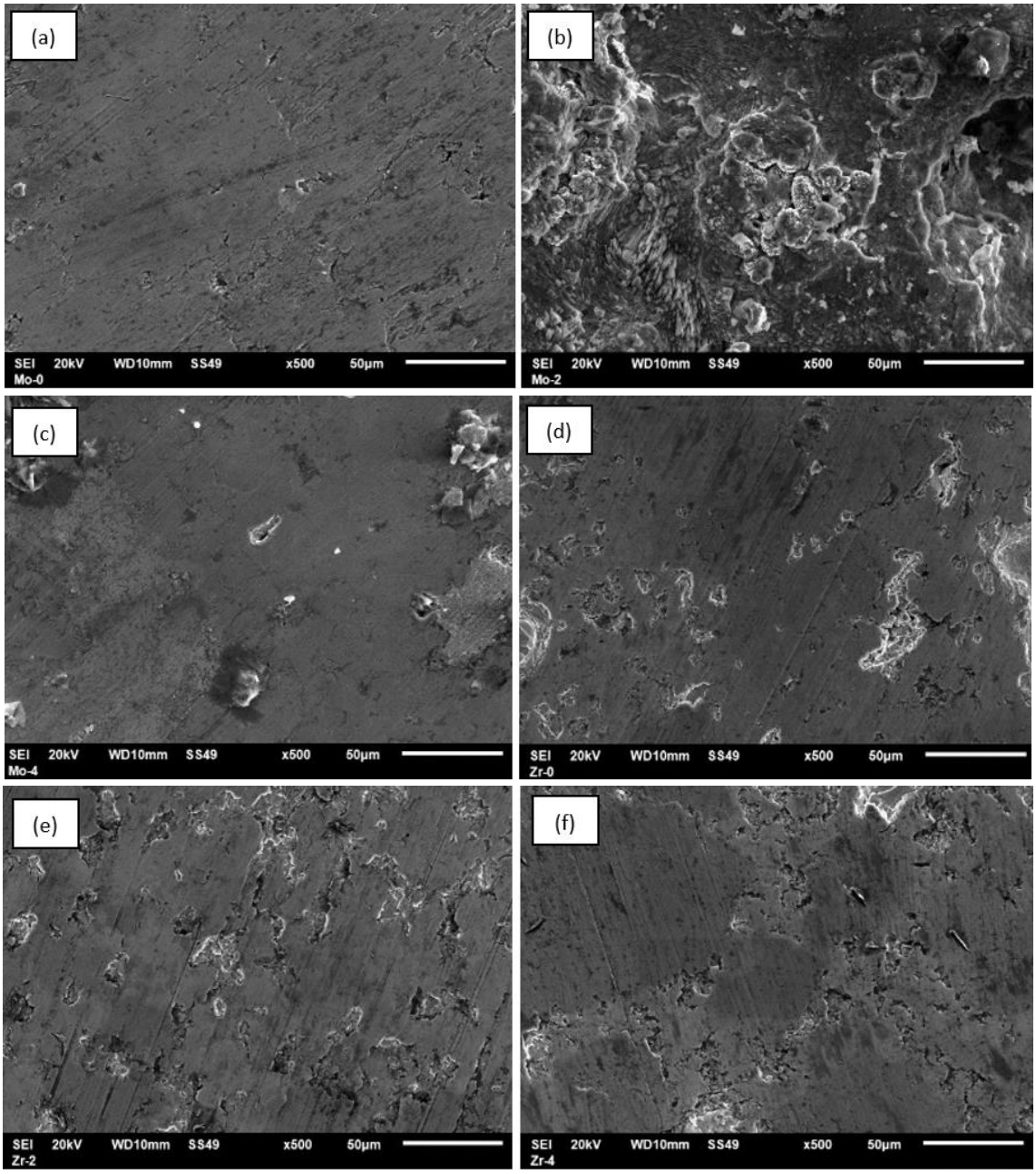

Figure 1. Microstructure of optical microscope results of HEA samples AlCrFeNiMo (a), $Al_{1.2}$CrFeNiMo (b), $Al_{1.4}$CrFeNiMo (c), AlCrFeNiZr (d), $Al_{1.2}$CrFeNiZr (e), $Al_{1.4}$CrFeNiZr (f).

Figure 2 shows the results of microstructure analysis of the HEA samples AlCrFeNiMo, Al1.2CrFeNiMo, Al1.4CrFeNiMo, AlCrFeNiZr, Al1.2CrFeNiZr, and Al1.4CrFeNiZr using SEM with 1000X magnification. The results of the microstructure analyzed by EDS to see the distribution of the elements on the surface of the sample which is shown in Table 4. The results of the microstructure analysis show dark gray, light gray and white colors, where the results of the microstructure were influenced by the distribution of the elements present on the alloy surface. Based on the results of the analysis, it is known that the dark gray color consists of the dominant Cr element as in the samples of AlCrFeNiMo, $Al_{1.4}$CrFeNiMo, and $Al_{1.4}$CrFeNiZr. The light gray color tends to be in samples with Zr element such as AlCrFeNiZr and $Al_{1.2}$CrFeNiZr samples. The white color formed on the surface of the alloy was composed of the dominant Mo element as in the $Al_{1.2}$CrFeNiMo sample.

DOI: 10.17146/urania.2021.27.2.6406

p ISSN: 0852-4777
e ISSN: 2528-0473

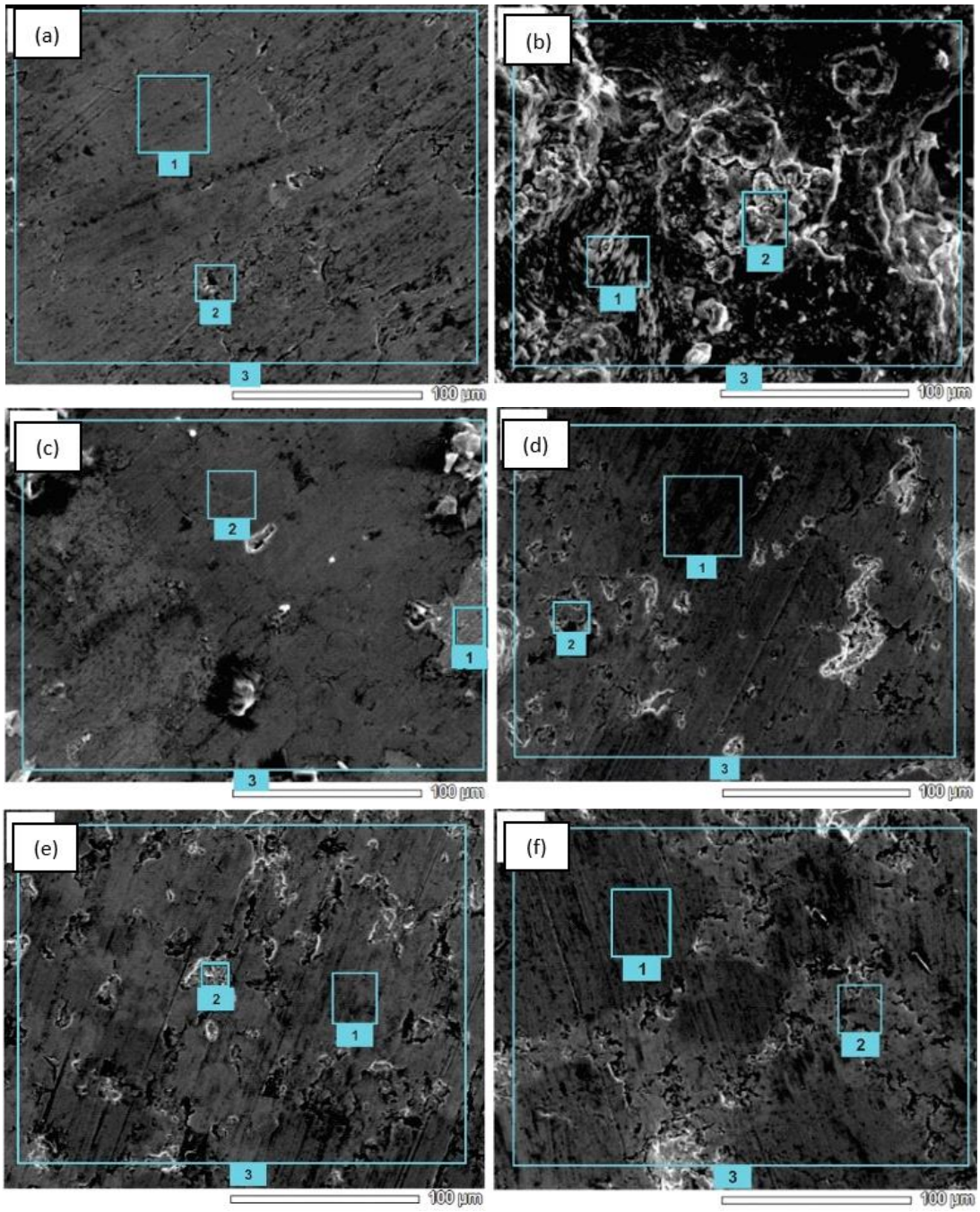

Figure 2. Results of SEM Analysis HEA samples AlCrFeNiMo (a), $Al_{1.2}$CrFeNiMo (b), $Al_{1.4}$CrFeNiMo (c), AlCrFeNiZr (d), $Al_{1.2}$CrFeNiZr (e), $Al_{1.4}$CrFeNiZr (f).

d. Hardness Test

Figure 3 shows the hardness values of the HEA samples AlCrFeNiMo, $Al_{1.2}$CrFeNiMo, $Al_{1.4}$CrFeNiMo, AlCrFeNiZr, $Al_{1.2}$CrFeNiZr, and $Al_{1.4}$CrFeNiZr. Based on the results of the hardness test, it was found that Al had a different effect on the HEA sample using Mo and Zr. In the HEA sample using Zr, it shows that with addition of Al, the hardness value of the sample increases this is due to the higher Al content caused the dislocations to be more difficult to move from one grain to another so that the hardness of the sample increases [16]. According to Tsai and Yeh [2] the addition of Al can affect the crystal structure, the higher of Al content tends to form crystal structure of BCC. According to Pickering et al [5] in their research, they explained that the BCC tends to have superior resistance than FCC because the defects

produced by BCC are less than FCC. Meanwhile, the HEA sample using Mo showed a decrease the hardness value in the sample with the addition of Al. According to Sriraman et al [17], this is influenced by the crystallite size of the alloy, where the crystallite size value is inversely proportional to the hardness value, the larger of crystallite size has lowest hardness value and conversely smaller of crystallite size has the higher hardness value as shown in Table 2. The hardness was obtained also influenced by the phase formed in the alloy. Based on the results of the Rietveld analysis in Table 3, it shows that the percentage of the AlNi phase decreased trend as the Al value increased in samples using the Mo element and the AlCrNi phase increased as Al value increased. AlNi and AlCrNi are phases with BCC structure which have better mechanical properties than FCC and HCP structures that can make good hardness properties on the alloy [5][12][18].

Table 4. Data on the distribution of HEA sample elements

HEA	Point	Weight (%)
AlCrFeNiMo	1	Al (2.1), Cr (84.4) Fe (4.3), Ni (7.0), Mo (2.04)
	2	Al (9.7), Cr (39.3), Fe (5.7), Ni (28.7) Mo (16.5)
	3	Al (6.9), Cr (55.9), Fe (11.3), Ni (23), Mo (2.7)
$Al_{1.2}CrFeNiMo$	1	Al (9.2), Cr (1.8), Fe (4.3), Ni (16), Mo (68.5)
	2	Al (30.8), Cr (1.4), Fe (7.4), Ni (34.9) Mo (25.35)
	3	Al (26.5), Cr (4.5), Fe (7.7), Ni (19.2) Mo (41.9)
$Al_{1.4}CrFeNiMo$	1	Al (0.3), Cr (0.28), Fe (0.37), Ni (0), Mo (98.9)
	2	Al (21.8), Cr (16), Fe (25), Ni (26.8) Mo (9.9)
	3	Al (17.9), Cr (12), Fe (17.4), Ni (23) Mo (29)
AlCrFeNiZr	1	Al (18.8), Cr (13), Fe (12.4), Ni (43), Zr (12)
	2	Al (7.7), Cr (5.3), Fe (19), Ni (18.6) Zr (49.3)
	3	Al (7.8), Cr (23.5) Fe (20), Ni (22.7) Zr (25.4)
$Al_{1.2}CrFeNiZr$	1	Al (5.8), Cr (1.3), Fe (5.2), Ni (21.2) Zr (66.2)
	2	Al (11.1), Cr (0.7), Fe (3.5), Ni (28.8) Zr (55.6)
	3	Al (6.8), Cr (15.5), Fe (11.2), Ni (17) Zr (49.1)
$Al_{1.4}CrFeNiZr$	1	Al (1.6), Cr (91.3), Fe (3.9), Ni (0.7) Zr (2.2)
	2	Al (9.9), Cr (4.3), Fe (41.8), Ni (13) Zr (30.9)
	3	Al (7.9), Cr (45.8), Fe (14.2), Ni (10) Zr (21.7)

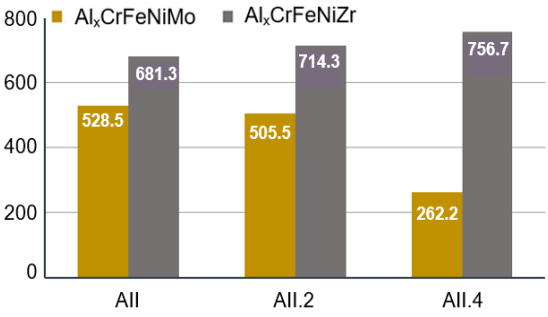

Figure 3. Hardness values of AlCrFeNiMo, $Al_{1.2}CrFeNiMo$, $Al_{1.4}CrFeNiMo$, AlCrFeNiZr, $Al_{1.2}CrFeNiZr$, and $Al_{1.4}CrFeNiZr$ HEA samples

e. Analysis of Corrosion Rate

Figure 4 shows polarization curve of samples AlCrFeNiMo, $Al_{1.2}CrFeNiMo$, $Al_{1.4}CrFeNiMo$, AlCrFeNiZr, $Al_{1.2}CrFeNiZr$, and $Al_{1.4}CrFeNiZr$ in 3wt% NaCl solution. Based on the potentiostat test, the corrosion potential (E_{corr}) and current density (I_{corr}) that obtained from the Tafel extrapolation, and calculation of corrosion rate are shows in Table 5. The results of the corrosion rate test show that the HEA $Al_{1.4}CrFeNiZr$ sample has the lowest corrosion rate of 0.20 mm/year. This proves that the Al content affects the corrosion resistance of HEA samples. Al has a function to increase corrosion resistance because it can form a protective passive layer. HEA samples that using Mo the corrosion rate increased this was due to the more aluminum passive layer formed, which causes depletion of other passive layers [19]. However, the Al content showed a significant effect on the corrosion resistance of HEA samples. Generally, the difference of corrosion rate of HEA samples using Mo and Zr elements is caused by the solubility of the alloy in 3wt% NaCl, Mo more soluble than Zr [20].

DOI: 10.17146/urania. 2022.28.1.6624

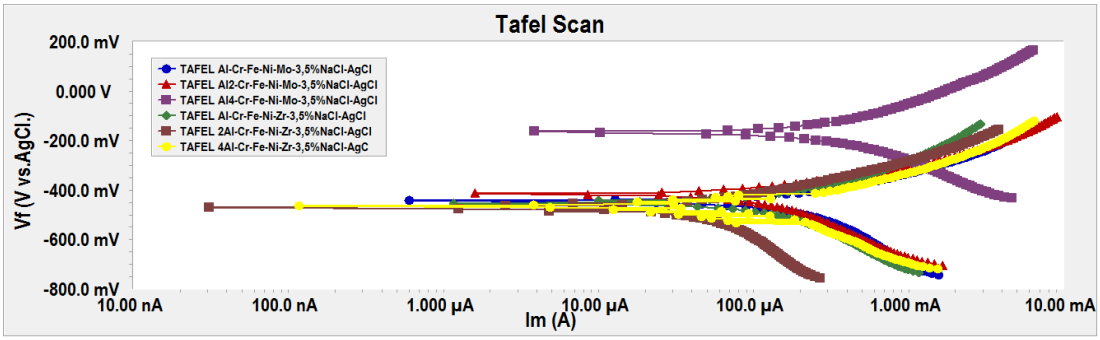

Figure 4. Potentiodynamic polarization curve of AlCrFeNiMo, $Al_{1.2}$CrFeNiMo, $Al_{1.4}$CrFeNiMo, AlCrFeNiZr, $Al_{1.2}$CrFeNiZr, and $Al_{1.4}$CrFeNiZ in 3wt% NaCl solution.

Table 5. The corrosion rate of HEA samples

Sample HEA	I_{corr} µA/cm^2	E_{corr} mV	Corrosion Rate mm/year
AlCrFeNiMo	174.0	-442.0	1.70
$Al_{1.2}$CrFeNiMo	113.0	-414.0	1.10
$Al_{1.4}$CrFeNiMo	251.0	-164.0	2.40
AlCrFeNiZr	127.0	-453.0	1.21
$Al_{1.2}$CrFeNiZr	25.9	-472.0	0.24
$Al_{1.4}$CrFeNiZr	21.4	-464.0	0.20

CONCLUSIONS

Samples of HEA AlCrFeNiSi, $Al_{1.2}$CrFeNiSi, and $Al_{1.4}$CrFeNiSi, were successfully produced by powder metallurgy process and sintering at 1000^{o}C. The results of the hardness test showed that the $Al_{1.4}$CrFeNiZr sample had the highest hardness value of 756.7 HV and the $Al_{1.4}$CrFeNiMo sample had the lowest hardness of 262.2 HV. The results of the corrosion test of the HEA sample showed that the HEA samples with Zr element has good corrosion resistance than HEA sample with Mo element.

ACKNOWLEDGMENTS

These works are under the project to develop nuclear fuel for research reactor in Research Center for Nuclear Fuel Cycle Technology and Radioactive Waste, Research Organization for Nuclear Energy - BRIN.

REFERENCES

[1]. I. Husnayani, M. B. Setiawan, P. M. Udiyani, and S. Kuntjoro, “Evaluation of nuclear heating in sample materials irradiated in RSG-GAS core,” *AIP Conference Proceedings.* vol. 2180, 2019. doi: 10.1063/1.5135520.

[2]. M. H. Tsai, and J. W. Yeh, “High-entropy alloys: A critical review. *Mater. Res. Lett.*, vol. 2, no. 3, pp. 107–123, 2014. doi: 10.1080/21663831.2014.912690.

[3]. N. Jaksic, V. Radu, and F. K. Nilsson, “Nuclear fuel cladding review of the zircaloy cladding and basic analysis of the model with the single hydride,” *Directorate General Joint Research Centre, Institute for Energy*, 2008.

[4]. D. B. Miracle, J.D. Miller, O. N. Senkov, C. Woodward, M . D. Uchic, and J. Tiley, “Exploration and development of high entropy alloys for structural applications,” *Entropy*, vol. 16, no. 1, pp. 494–525, 2014. doi: 10.3390/e16010494.

[5]. E. J. Pickering, A.W. Carruthers, P. J. Barron, S. C. Middleburgh, D. E. J. Armstrong, and A. S. Gandy, “High-entropy alloys for advanced nuclear applications,” *Entropy*, vol. 23, no. 1, pp. 1–28, 2021. doi: 10.3390/e23010098.

[6]. Y. Shi, B. Yang, and P. K. Liaw, “Corrosion-resistant high-entropy alloys: A review,” *Metals (Basel).*, vol. 7, no. 2, pp. 1–18, 2017. doi: 10.3390/met7020043.

[7]. X. Wang, W. Guo, and Y. Fu, “High-entropy alloys: Emerging materials for advanced functional applications,” *J. Mater. Chem. A.*, vol. 9. no. 2. pp. 663–701, 2021. doi: 10.1039/d0ta09601f.

[8]. J. Setiawan, S. Pribadi, A. Jamaludin, Sungkono and M. H. Al-Hasa, “Structural analysis of Al alloys for nuclear fuel cladding,” *AIP Conference Proceedings.* vol. 2262, 2020. doi: 10.1063/5.0015710.

[9]. D. M. Rodríguez, F. Plazaola, J. S. Garitaonandia, J. A. Jiménez, and E. Apiñaniz, “Influence of volume and Fe local environment on magnetic properties of Fe-rich Fe-Al alloys. *Intermetallics*, vol. *24*, pp. 38–49, 2012. https://doi.org/10.1016/j.intermet.2012.01.021

[10]. Masruroh, A. B. Manggara, T. Lapailaka, dan R. Triandi, "Penentuan ukuran kristal (crystallite size) lapisan tipis pzt dengan metode XRD melalui pendekatan persamaan debye scherrer, "*Erudio Journal of Educational Innovation*, vol. *1, no.2*, hal. 24–29, 2013. https://doi.org/10.18551/erudio.1-2.4

[11]. O. A. Cortez, F. J. Moura, E. A. Brocchi, R. C. S. Navarro and R. M. S. Fernandes, "Fe-Ni Alloy Synthesis Based on Nitrates Thermal Decomposition Followed by H2 Reduction," *Metall. Mater. Trans. B Process Metall. Mater. Process. Sci.*, vol. 45, no. 6, pp. 2033–2039, 2014. doi: 10.1007/s11663-014-0221-x.

[12]. T. Davey, N. D. Tran, A. Saengdeejing, and Y. Chen, "First-principles-only CALPHAD phase diagram of the solid aluminium-nickel (Al-Ni) system," *Calphad: Computer coupling of phase diagrams thermochemistry*, vol. 71, p. 102008, 2020. doi: 10.1016/j.calphad. 2020.102008.

[13]. B. Grushko, W. Kowalski, D. Pavlyuchkov, B. Przepiórzyński, and M. Surowiec "A contribution to the Al-Ni-Cr phase diagram," *J. Alloys Compd.*, vol. 460, no. 1–2, pp. 299–304, 2008. doi:10.1016/j.jallcom.2007.06.044.

[14]. D. M. Kondrat'ev, K. B. Kalmykov, N. E. Dmitrieva, and S. F. Dunaev, "Phase equilibria in Al-Ni-Zr system at 1123 K," *Moscow Univ. Chem. Bull.*, vol. 67, no. 6, pp. 259–264, 2012. doi: 10.3103/S0027131412060053.

[15]. Y. J. An, L. Zhu, S. Jin, J. Lu, and X. Liu, "Laser-ignited self-propagating sintering of AlCrFeNiSi high-entropy alloys: An improved technique for preparing high-entropy alloy," *Metals*, vol. 9, no. 4, pp. 1–9, 2019. doi:10.3390/met9040438.

[16]. E. Nugroho, "Pengaruh unsur aluminium dalam kuningan terhadap kekerasan, kekuatan tarik, dan struktur mikro," *Turbo: Jurnal Program Studi Teknik Mesin*, vol. 1, no. 10, pp. 10–15, 2012. doi: 1. 10.24127/trb.v1i1.82

[17]. K. R. Sriraman, S. G. S. Raman, and S. K. Seshadri, "Influence of crystallite size on the hardness and fatigue life of steel samples coated with electrodeposited nanocrystalline Ni-W alloys," *Materials Letter.* vol. 61, no. 3, pp. 715–718, 2007. doi: 10.1016/j.matlet.2006.05.049.

[18]. Y. Wang, and G. Cacciamani, "Thermodynamic modeling of the Al-Cr-Ni system over the entire composition and temperature range," *Journal of Alloys and Compounds*, vol. *688*, pp. 422–435, 2016. https://doi.org/10.1016/j. jallcom.2016. 07.130

[19]. Y. Shi, B. Yang, X. Xie, J. Brechtl, K. A. Dahmen, and P. K. Liaw, "Corrosion of Al xCoCrFeNi high-entropy alloys: Al-content and potential scan-rate dependent pitting behavior," *Corrosion Science.* vol. 119, pp. 33–45, 2017. doi: 10.1016/j.corsci.2017.02.019.

[20]. M. K. Ajiriyanto, D. Anggraini, and R. Kriswarini, "Analisis korosi paduan ZIRLO-Mo dalam media NaCl menggunakan metode polarisasi," *Urania J. Ilm. Daur Bahan Bakar Nukl.*, vol. 23, no. 3, pp. 183–194, 2017. doi: 10.17146/urania.2017.23.3.3221.